ARTICLE

Pilot scale production and characterization of next generation high molecular weight and tense quaternary state polymerized human hemoglobin

Clayton T. Cuddington [ORCID] | Savannah R. Wolfe | Donald A. Belcher [ORCID] |
Megan Allyn | Alisyn Greenfield | Xiangming Gu [ORCID] | Richard Hickey |
Shuwei Lu | Tanmay Salvi | Andre F. Palmer

William G. Lowrie Department of Chemical
and Biomolecular Engineering, The Ohio State
University, Columbus, OH, USA

Correspondence
Andre F. Palmer, William G. Lowrie
Department of Chemical and Biomolecular
Engineering, The Ohio State University, 452
CBEC, 151 West Woodruff Ave, Columbus,
OH 43210, USA.
Email: palmer.351@osu.edu

Abstract

Polymerized human hemoglobin (PolyhHb) is being studied as a possible red blood cell (RBC) substitute for use in scenarios where blood is not available. While the oxygen (O_2) carrying capacity of PolyhHb makes it appealing as an O_2 therapeutic, the commercial PolyhHb PolyHeme® (Northfield Laboratories Inc.) was never approved for clinical use due to the presence of large quantities of low molecular weight (LMW) polymeric hemoglobin (Hb) species (<500 kDa), which have been shown to elicit vasoconstriction, systemic hypertension, and oxidative tissue injury in vivo. Previous bench-top scale studies in our lab demonstrated the ability to synthesize and purify PolyhHb using a two-stage tangential flow filtration purification process to remove almost all undesirable Hb species (>0.2 μm and <500 kDa) in the material, to create a product that should be safer for transfusion. Therefore, to enable future large animal studies and eventual human clinical trials, PolyhHb synthesis and purification processes need to be scaled up to the pilot scale. Hence in this study, we describe the pilot scale synthesis and purification of PolyhHb. Characterization of pilot scale PolyhHb showed that PolyhHb could be successfully produced to yield biophysical properties conducive for its use as an RBC substitute. Size exclusion high performance liquid chromatography showed that pilot scale PolyhHb yielded a high molecular weight Hb polymer containing a small percentage of LMW Hb species (<500 kDa). Additionally, the auto-oxidation rate of pilot scale PolyhHb was even lower than that of previous generations of PolyhHb. Taken together, these results demonstrate that PolyhHb has the ability to be seamlessly manufactured at the pilot scale to enable future large animal studies and clinical trials.

KEYWORDS

hemoglobin-based oxygen carrier, pilot scale synthesis, polymerized human hemoglobin, process scaleup, red blood cell substitute, therapeutic

1 | INTRODUCTION

Allogenic blood transfusion is the most definitive treatment for blood loss (Greenburg, 1996). Unfortunately, the American Red Cross is experiencing one of the worst blood shortages in over a decade because of the COVID-19 pandemic (American Red Cross, 2022a). This has caused deferment of life-saving procedures such as organ transplants for some patients (American Red Cross, 2022b). Unfortunately, blood shortages are not limited to pandemics, and can occur seasonally and during other crises such as natural disasters or wars (Glynn et al., 2003). In these scenarios, blood availability may not meet the demand for blood, or blood may not be available near to the trauma site (Stowell et al., 2001). To address these challenges, there needs to be alternatives to blood that can keep an individual alive to bridge the gap between blood loss and definitive blood transfusion.

Given the scarcity of blood, the current standard of care administered by emergency personnel involves transfusion of crystalloid or colloid solutions to maintain mean arterial pressure and blood volume (Holcomb et al., 2015; Myburgh et al., 2012). These emergency transfusions are only meant to alleviate the immediate effects of hypovolemic shock and do not provide oxygen (O_2) to tissues, unlike blood (Cabrales et al., 2007). Therefore, hemoglobin (Hb)-based O_2 carriers (HBOCs) are actively being developed as an alternative to crystalloid or colloid solutions as a red blood cell (RBC) substitute to replace lost blood volume (Moore et al., 2009). HBOCs are able to resuscitate hypoxic tissues, which is facilitated by Hb's innate ability to bind and release O_2 (G. Chen & Palmer, 2009). A solution of acellular (cell-free) Hb cannot be used in transfusion medicine as a suitable HBOC, since the protein is small enough (64 kDa) to extravasate through the endothelial cell–cell junction pores lining the blood vessel wall into the tissue space (Bucci et al., 2008). As a result, cell-free Hb scavenges nitric oxide (NO), eliciting vasoconstriction and systemic hypertension (Cullison et al., 2019; Gibson & Roughton, 1956; Kavdia et al., 2002; McCarthy et al., 2001; Winslow, 2007). In addition, Hb deposition into the tissue space leads to oxidative tissue injury (Butt et al., 2011).

To mitigate the cytotoxic effects of cell-free Hb, HBOCs require modification of Hb via processes such as chemical crosslinking or particle encapsulation to generate a molecule/particle large enough to prevent tissue extravasation, while still maintaining Hb's native O_2 transport properties (Kim & Greenburg, 2004; Silverman & Weiskopf, 2009). Polymerized Hb (PolyHb) is the most well-studied HBOC and typically uses glutaraldehyde as a nonspecific Hb crosslinker (Alayash, 2000; Alayash et al., 2001; Chang, 1971; Chang et al., 2021; Guillochon et al., 1981, 1986). PolyHeme® (Northfield Laboratories Inc.), Hemopure® (HbO₂ Therapeutics), and Hemolink® (Hemosol) are all commercial PolyHbs that failed phase III clinical trials (J. Y. Chen et al., 2009). These HBOCs are mostly composed of low molecular weight (LMW) Hb species (<500 kDa) that pose similar side-effects to cell-free Hb, thus resulting in their failure in clinical trials (Buehler et al., 2010; Harris & Palmer, 2008; Zhang et al., 2011).

Thus, despite their clinical potential, there are still no FDA approved HBOCs for use in transfusion medicine (Chang et al., 2021).

To minimize the adverse side-effects observed in PolyHb clinical trials derived by the presence of LMW Hb species, previous work in our lab focused on removing the LMW Hb species from the PolyHb product via tangential flow filtration (TFF) (Cuddington et al., 2021). Building on the prior success of our bench-top scale polymerized human Hb (PolyhHb) synthesis protocol that can produce 15 g of PolyhHb in one batch, the current study focuses on scaling up PolyhHb production to the 200–300 g scale that brackets PolyhHb between 500 kDa and 0.2 μm, therefore removing the majority of LMW Hb species that elicit vasoconstriction, systemic hypertension, and oxidative tissue injury; as well as, any high molecular weight (HMW) species over 0.2 μm in size that could signal the reticulo-endothelial system (RES) to quickly clear the material from the circulation (Cuddington et al., 2021; Gaur et al., 2000; Gustafson et al., 2015). Therefore, PolyhHb scaleup is essential to enable safety and efficacy studies in large animals before subsequent evaluation in humans.

In this study, PolyhHb scaleup followed a protocol mirroring the PolyhHb bench-top synthesis parameters outlined in the literature (Cuddington et al., 2021). The scale of production was increased from our published 1.5 L bench-top scale reactor system to a 30 L pilot-scale reactor system. The use of TFF modules enabled scalable purification of PolyhHb (Pires & Palmer, 2021). Therefore, this study describes the synthesis and characterization of pilot scale PolyhHb produced in both the low and moderate O_2 affinity state and compares the pilot scale PolyhHb product to previously published bench-top scale PolyhHb product.

2 | MATERIALS AND METHODS

2.1 | Materials

Sodium dithionite ($Na_2S_2O_4$), glutaraldehyde ($C_5H_8O_2$) (70 wt%), sodium cyanoborohydride ($NaCNBH_3$), sodium lactate ($NaC_3H_5O_3$), N-acetyl-L-cysteine (NALC, $C_5H_9NO_3S$), and calcium chloride dihydrate ($CaCl_2·2H_2O$) were purchased from Sigma Aldrich. Sodium chloride (NaCl), potassium chloride (KCl), sodium phosphate monobasic (NaH_2PO_4), sodium phosphate dibasic (Na_2HPO_4), sodium hydroxide (NaOH), and 0.2 μm Titan3 sterile filters were purchased from Fisher Scientific. Hollow fiber tangential flow filtration (TFF) modules N02-P500-05-N (polysulfone [PS], 500 kDa pore size), N02-S20U-05-N (polyethersulfone [PES], 0.2 μM pore size), and N02-E65U-07-N (PES, 0.65 μM pore size) were purchased from Repligen. The Liqui-Cel™ EXF Series G420 Membrane Contactor was purchased from 3M. A minicentrifuge (50-090-100, with a working speed of 6000 rpm and maximum speed of 6600 rpm) was obtained from Fisher Scientific. Expired human leukoreduced, packed RBC units were acquired from Transfusion Services at the Wexner Medical Center, Canadian Blood Services, and Zen-Bio Inc.

2.2 | RBC washing process

One hundred and eighty liters of 0.9 wt% saline was prepared the night before the start of the RBC washing process. To prepare the saline, a vessel was first filled with 176 L of deionized (DI) water followed by the addition of 4 L of 40.5 wt% saline. The vessel was then stirred for 30 min and stored at 4°C. For each batch of pooled RBCs, a total of 18 RBC units were used in the washing process. Initially, the system vessel was primed with 0.9 wt% saline before addition of the RBC units. All RBC units were gently inverted and massaged to properly mix blood bag contents and then transferred into a 20 L Nalgene container in a biosafety cabinet and an initial pooled sample of RBCs was taken for analysis. The vessel was then transferred into a chromatography refrigerator, where it was maintained at 4°C for the entirety of the RBC washing process. The vessel containing pooled RBCs was diluted with 0.9 wt% saline to a hematocrit (HCT) of 22 ± 2% to reduce the RBC solution viscosity and standardize the HCT between replicates. Once the HCT was confirmed, the permeate line in the TFF RBC washing system (Figure 1) was opened to initiate the diafiltration (i.e., RBC washing) process. The diluted RBC solution underwent six system volume exchanges (diacycles) over a 0.65 μm mPES TFF cartridge with 0.9 wt% saline as the wash solution as shown in Figure 1. Retentate and permeate samples were taken after each diacycle, using a sample port in the retentate line to obtain the retentate sample, while permeate samples were collected from the permeate line entering a waste vessel.

2.3 | HCT quantification

RBC solution HCT was determined by loading 65 μl of the retentate sample into a 75 mm mylar wrapped capillary tube (Drummond) followed by centrifugation in a Sorvall Legend micro 17 microcentrifuge (Fisher Scientific) at 17g for 5 min. The HCT was determined using a standardized HCT calibration curve.

2.4 | RBC concentration quantification

The RBC concentration of retentate samples taken during the RBC wash process was measured using a Multisizer 4e Coulter Counter (Beckman Life Sciences). RBC samples were diluted 100× followed by the addition of 100 μl of the diluted sample into 20 ml of filtered Isoton solution (Beckman Life Sciences) for RBC concentration analysis in the Coulter Counter.

2.5 | hHb quantification

The cell-free hHb concentration in both permeate and retentate samples from the RBC wash process was measured using UV-visible absorbance spectrometry on a diode array spectrophotometer HP 8452 A (Olis). Retentate samples were first centrifuged on a minicentrifuge (Fisher Scientific) at 6000 rpm for 2 min, followed by removal of the supernatant for spectrometry measurements. The supernatant hHb concentration

RBC Wash Procedures:
1. RBCs at 22 ± 2% HCT were washed with saline over a 0.65 μm TFF filter
2. Retentate & permeate samples were collected every diacycle

hHb Purification Procedures:
3. RBCs were lysed with PB (3.75 mM, pH 7.4)
4. Membrane fragments were removed with a 500 kDa TFF filter
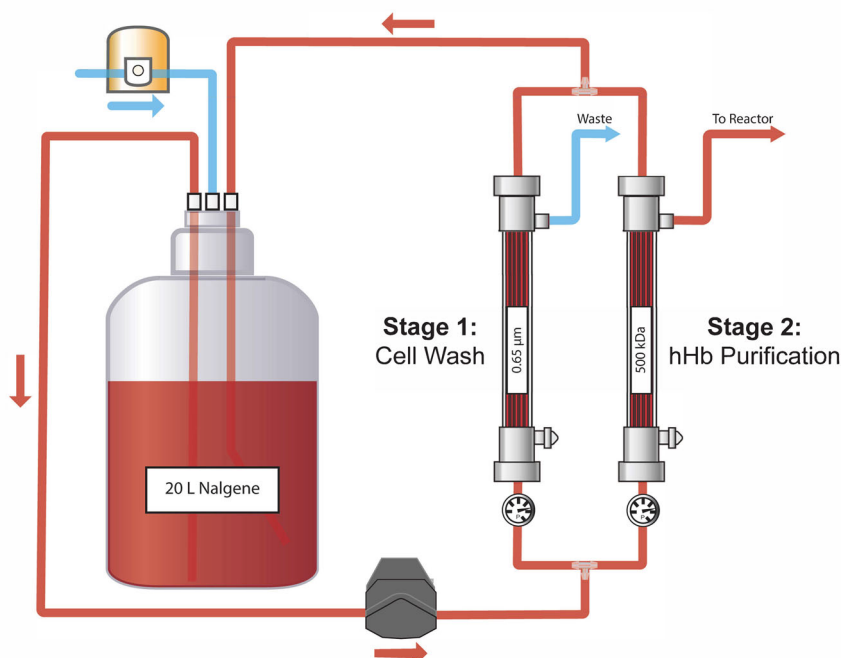5. Purified hHb was transferred to bioreactor

Waste   To Reactor

Stage 1: Cell Wash   0.65 μm   500 kDa   Stage 2: hHb Purification

20 L Nalgene

FIGURE 1 Diagram of the cell wash and human hemoglobin (hHb) purification process. Red blood cells (RBCs) are first washed over a 0.65 μm tangential flow filtration (TFF) module with cell-free hHb and cell debris permeating into the waste. After six diacycles of cell wash, the vessel is filled with phosphate buffer to lyse the intact RBCs. The lysate is then passed through the 500 kDa TFF module to obtain purified hHb which is then used to synthesize polymerized hHb (PolyhHb).

was analyzed by the cyanomethemoglobin method (Arifin & Palmer, 2003).

2.6 | hHb purification

After RBC washing via TFF, RBCs were lysed with phosphate buffer (PB) (3.75 mM, pH 7.4) for 1 h at 4°C with constant stirring. Lysed RBC membrane fragments and large aggregates were removed using a 500 kDa TFF module (Figure 1). Purified hHb and other RBC proteins <500 kDa were transferred into the stirred reactor shown in Figure 2. Hb purity has been shown to be >98% by densiometric analysis of SDS-PAGE gels in a prior TFF hHb purification study (Palmer et al., 2009). Once 480 g of hHb was loaded into the reactor vessel, a 2 L NaCl charge was added to convert the PB into phosphate-buffered saline (PBS). The hHb in the reactor was recirculated through a gas contactor loop in addition to having a nitrogen (N_2) head space in the reactor to deoxygenate the protein. The hHb solution was left to deoxygenate overnight at 14°C using a cooling coil system to limit methemoglobin (metHb) formation.

2.7 | hHb polymerization

The next day, the hHb solution in the reactor was brought up to physiological temperature (37°C) using a thermal jacket wrapped around the reactor. The pO_2 of the system was checked periodically using a RAPIDLab 248 blood gas analyzer (Siemens) with the goal of achieving a pO_2 value of 0.0 ± 2.0 mmHg before hHb polymerization to achieve 100% tense quaternary state (T-state) hHb and PolyhHb. To ensure complete hHb deoxygenation, sodium dithionite was added in 1 g charges until a pO_2 of 0 mmHg was achieved.

Once the hHb in the reactor was fully deoxygenated, the gas contactor was temporarily bypassed to begin hHb polymerization as shown in Figure 2. Polymerization was performed with approximately a 30:1 molar ratio of glutaraldehyde (GA) to hHb. The volume of GA was diluted in 3 L of PBS (pH 7.4) and bubbled with N_2. The solution

Hemoglobin Polymerization Reactor Components:

1. 30 L Dished Bottom Reactor Vessel
2. Pitched Blade Impeller
3. Cooling Coil
4. Heating Jacket
5. Temperature Controller
6. Seal Kit
7. Cooling Water Inlet
8. Cooling Water Outlet
9. Impeller Rotor
10. Gas Vent
11. Thermal Couple
12. O_2 Impermeable Tubing
13. Masterflex® I/P® Series Peristaltic Pump
14. Membrane Contactor
15. Sweep Gas Inlet
16. Sweep Gas Outlet
17. 1.5 L Tinted Glass Bottle
18. Masterflex® L/S® Series Peristaltic Pump
19. Sampling Valve
20(a,b,c,d). Pressure Clip
21. Floor Scale with Ramp
22(a,b). Three-way Valve
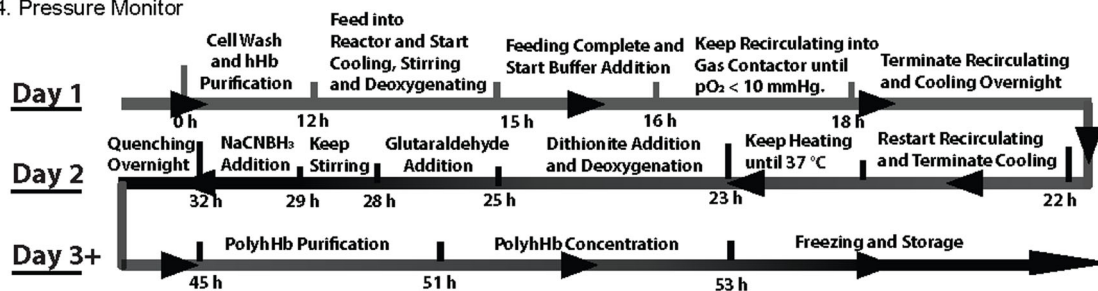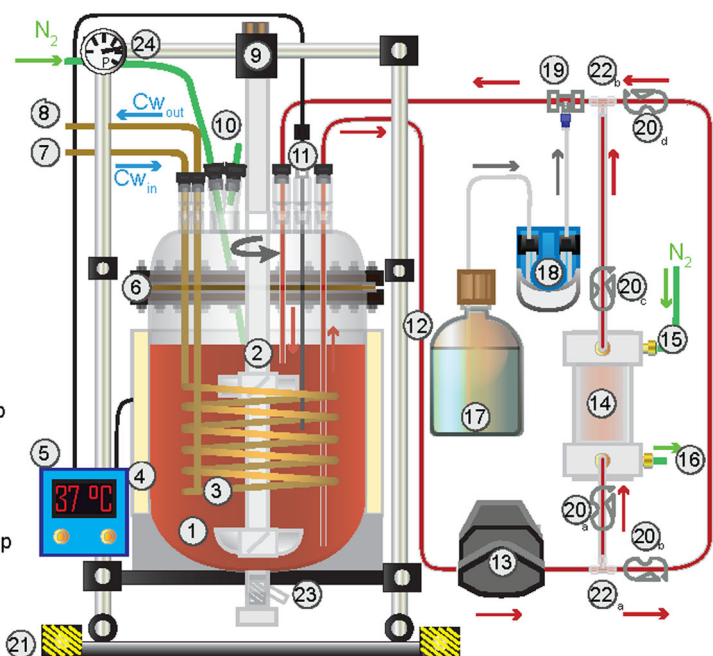23. Draining Port
24. Pressure Monitor

FIGURE 2 Diagram of the reactor system used for the human hemoglobin (hHb) polymerization process. The reactor was filled with purified hHb on Day 1, polymerized with glutaraldehyde and subsequently quenched with NaCNBH₃ on Day 2 and transferred into the PolyhHb TFF purification process (Figure 3) on Day 3.

was then pumped into the reactor over 3 h followed by an additional hour of reaction time. A N_2 head space was maintained in the reactor and the GA solution vessel. Following the hHb polymerization reaction, the heating jacket was removed, and the cooling coils were turned on. The system was quenched with a 7:1 molar ratio of $NaCNBH_3$ to GA, diluted in 3 L of PBS (pH 7.4). The quenching solution was added to the reactor over a period of 10 min. The system was monitored for at least 30 min before being held at 14°C overnight. Throughout the hHb polymerization process, the impeller speed was maintained at approximately 130 rpm and turned off during the overnight hold time.

2.8 | PolyhHb separation and purification

Following the hHb polymerization process, the PolyhHb solution was pumped from the reactor to a Stage 1 PolyhHb purification vessel operated inside a chromatography refrigerator as shown in Figure 3. The Stage 1 recirculation loop passed the PolyhHb solution through a 0.2 μm PES TFF cartridge into a Stage 2 PolyhHb purification vessel as shown in Figure 3, with undesired particulates or HMW polymerized material being retained in Stage 1 (>0.2 μm). The Stage 2 recirculation loop facilitated excipient exchange of the PolyhHb solution over a 500 kDa PS TFF cartridge with a modified Ringer's lactate solution. This was performed to both remove LMW Hb polymeric species (<500 kDa), unmodified cell-free hHb, and free reactants from the final product as well as to exchange the PolyhHb from the PBS buffer to a more physiologically relevant crystalloid (modified Ringer's lactate). At least 12 full diacycles were performed to ensure the final PolyhHb solution contained <5% LMW Hb species (<500 kDa). Once the excipient exchange was completed, the final PolyhHb product was concentrated over the 500 kDa TFF filter to >10 g/dl. The final protein concentration and metHb level were

measured using the cyanomethemoglobin method (Arifin & Palmer, 2003). The final PolyhHb product was stored at −80°C until use (Cuddington et al., 2020).

2.9 | Oxygen equilibrium curve

A Hemox Analyzer (TCS Scientific Corp.) was used to measure the oxygen equilibrium curve (OEC) of hHb and PolyhHb. The OEC was fit to the Hill equation to regress the cooperativity coefficient (n_H) and partial pressure of O_2 at which 50% of the hHb or PolyhHb was saturated with O_2 (P_{50}).

2.10 | Polymer molecular weight (MW) and size

The MW distribution of hHb and PolyhHb was measured using size exclusion chromatography (SEC) on a high-pressure liquid chromatography (HPLC) system. The separation was performed using an Ultimate 3000 system with an SEC-1000 column (Thermo Fisher Scientific). The absorbance was measured at 412 nm to monitor the Soret peak characteristic of hHb (Cuddington et al., 2020). The hydrodynamic diameter of hHb and PolyhHb was measured using a Zetasizer Nano Dynamic Light Scattering (DLS) Spectrometer (Malvern Instruments).

2.11 | Auto-oxidation kinetics

UV-visible absorbance spectrometry was used to measure the auto-oxidation kinetics of hHb and PolyhHb. The hHb/PolyhHb solution was diluted in PB to 12.5 g/L to simulate the average concentration of product in the systemic circulation following transfusion
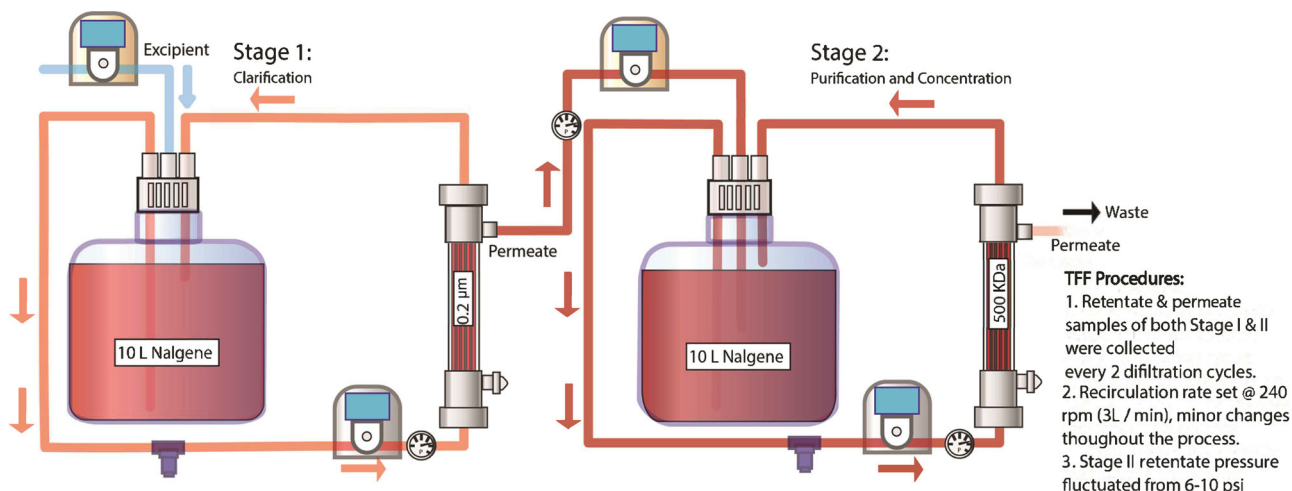

FIGURE 3 Diagram of the two-stage tangential flow filtration PolyhHb purification process. Stage 1 retains any polymers that are too large (>0.2 μm), and Stage 2 facilitates removal of unreacted chemicals and low molecular weight (LMW) hemoglobin (Hb) species from the system (<500 kDa). The PolyhHb is washed with >12 diacycles of a modified Ringer's lactate solution to remove the majority of LMW Hb species and to buffer exchange the PolyhHb into the modified Ringer's lactate solution.
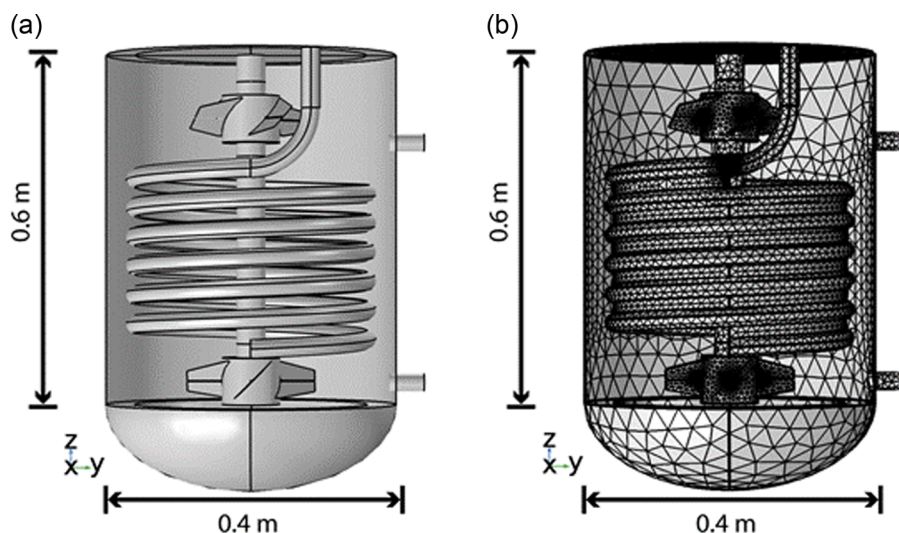
(a) (b)

FIGURE 4 Geometry and meshing of the continuous stirred tank reactor generated by Comsol 5.3a for the PolyhHb reactor.

(Jahr et al., 2008). The solution was monitored for 24 h, while maintaining a physiological temperature (37°C) and pH (7.40). The absorbance at 630 nm was monitored over a 24-h period. Analyzing the kinetics for hHb and PolyhHb, the fraction of heme in the ferrous state as a function of time was analyzed assuming first-order rate kinetics to regress the auto-oxidation rate constant (k_{ox}) in h^{-1}.

2.12 | Stopped-flow kinetics

A SX-20 micro-volume stopped-flow apparatus (Applied Photophysics) was used to measure the O_2 offloading kinetics and the haptoglobin (Hp) binding kinetics of hHb/PolyhHb. For the O_2 offloading kinetics, the absorbance at 437.5 nm was measured when a 12.5 μM (heme-basis) solution of oxygenated hHb/PolyhHb in PBS was rapidly mixed with a 1.5 g/L solution of sodium dithionite in degassed PBS. The average of the kinetic traces was fit to an exponential function using the Applied Photophysics software to regress the first-order O_2 dissociation rate constant ($k_{o2,off}$) in s^{-1}.

Hp binding kinetics was monitored by measuring the fluorescence emission at 310 nm when Hp binds to hHb/PolyhHb. A 5, 2.5, 1.25, and 0.625 μM solution of hHb/PolyhHb sample in PBS was rapidly mixed with a 0.25 μM solution of Hp. The average of the kinetic traces was fit to an exponential function and a pseudo-first-order rate constant was regressed at each concentration. The pseudo-first-order rate constants were plotted against hHb/PolyhHb concentration and fit to a linear function to regress the second-order Hp binding rate constant (k_{Hp-Hb}) in $μM^{-1} s^{-1}$.

2.13 | Computational methods

The fluid dynamics and mixing performance in the PolyhHb reactor vessel were modeled as a continuous stirred tank reactor (CSTR) and evaluated via Comsol Multiphysics (Version 5.3a; Comsol Inc.). In this study, the Rotating Machinery module was used to solve for the turbulent flow properties in the reactor. The simulated results were presented at steady state. Constant circulation of PolyhHb solution was maintained in between the inlet and outlet as shown in Figure 4 via a peristatic pump. The CSTR contained 2 four-bladed pitched impellers and a cooling coil. Fluid flow was evaluated using a stationary MUMPS solver with a relative tolerance of 1.0E−6 and automatic linearity. All simulations were conducted in 3D using a circular uniform distribution. The governing equations, mesh design, and relevant parameters are given in Supporting Information: Appendix A1.

2.14 | Statistical analysis

All data are presented as the mean ± standard deviation. Statistical analysis for data collected in the study was performed on RStudio using t-tests. For all tests, $p < 0.05$ was considered statistically significant.

3 | RESULTS AND DISCUSSION

3.1 | RBC wash process

The RBC wash process successfully removed the majority of cell-free Hb from the expired pooled RBC units while maintaining the more mechanically resilient RBCs for use in the subsequent hHb purification step of the pilot scale hHb polymerization process. Figure 5a shows that after four diacycles, the concentration of cell-free Hb in the permeate dropped below 0.5 g/L and remained constant for the remaining diacycles, verifying that the RBCs were thoroughly washed, while the more mechanically susceptible RBCs lysed and were removed from the system. Similarly, Figure 5b shows that after four diacycles, the concentration of cell-free Hb in the retentate remains below 2 g/L, which indicated that as much cell-free Hb was removed as possible from the system.
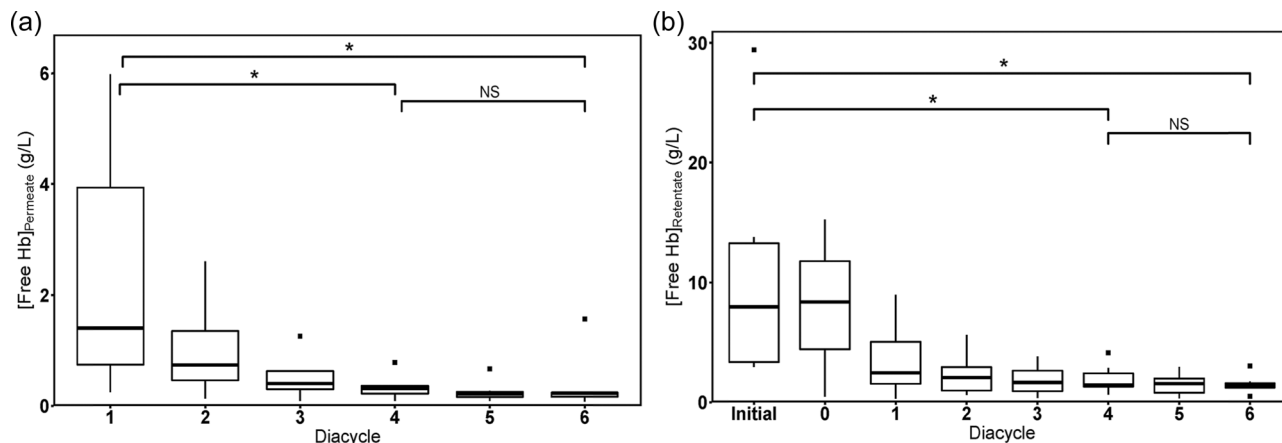
(a)

(b)

FIGURE 5 Hemoglobin (Hb) concentration during the tangential flow filtration-facilitated red blood cell (RBC) washing process. Concentration of cell-free Hb in the permeate stream (a) and concentration of cell-free Hb in the retentate vessel (b) monitored over six diacycles of the RBC washing process. The cell-free Hb concentration decreased significantly over four diacycles in both the retentate and the permeate and remained constant from diacycle 4 to 6. Outliers are shown as black squares. A total of five replicates were used.
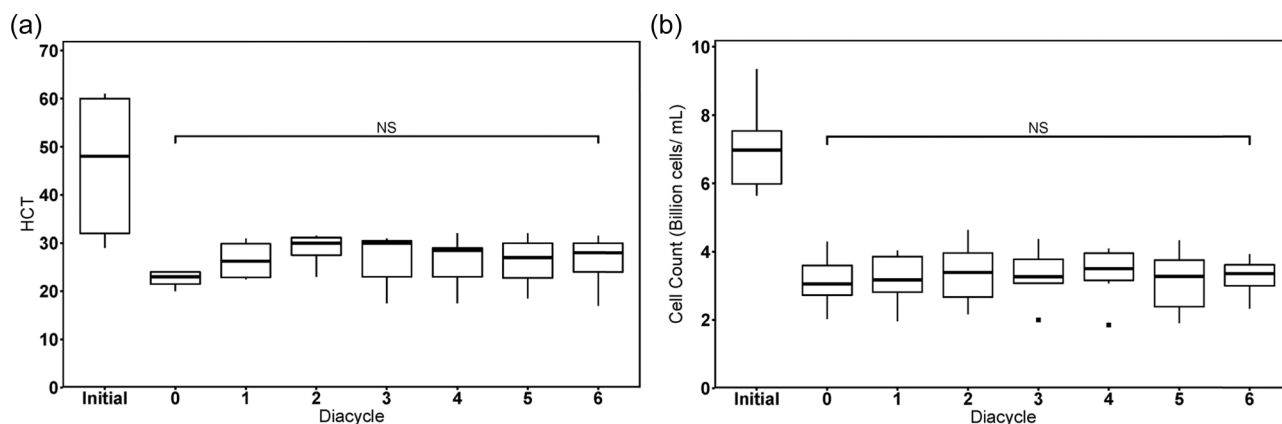
(a)

(b)

FIGURE 6 Hematocrit (HCT) and red blood cell (RBC) concentration during the tangential flow filtration-facilitated RBC washing process. HCT of the pooled RBC solution (a) and cell concentration (b) over six diacycles of the RBC washing process. For both the HCT and cell concentration, there was no significant difference between diacycles, indicating that there was no significant cell lysis throughout the RBC washing process. Outliers are shown as black squares. A total of five replicates were used.

The HCT is defined as the volume fraction of packed RBCs present in the RBC solution and is directly related to the concentration of RBCs in a well-mixed solution. In Figure 6a, the HCT was measured for the retentate after each washing diacycle to determine the volume fraction of intact RBCs present in the system volume during the RBC washing process. In recent work, we show that it is possible to wash RBCs with negligible hemolysis at physiological HCTs using a TFF system driven by a centrifugal pump. Conversely, peristaltic pumps are known to lyse cells traversing through the pump head due to tubing compression and subsequent pressure applied to the cells, which would decrease the HCT during the RBC washing process (Faghih & Sharp, 2019). However, in this study, the HCT remained constant ($p = 0.993$) as shown in Figure 6a after the initial HCT adjustment from the pooled packed RBC units to a HCT of 20%–24%, which indicated that with appropriate RBC dilution and application of a low pump speed, it is possible to wash RBCs with negligible loss due to shear-induced hemolysis.

The concentration of intact RBCs was then used to determine whether washing RBCs using TFF and subjecting RBCs to shear forces during the washing process is potentially detrimental to cell integrity and causes more unintentional hemolysis. No significant drop in RBC concentration was observed ($p = 0.999$) between the first and sixth diacycles as shown in Figure 6b, which further confirms the HCT measurements which indicated that there is negligible hemolysis during the RBC washing process at the selected pump speed and RBC dilution.

3.2 | PolyhHb quantification

Table 1 summarizes the various biophysical parameters measured in this pilot scale study as well as values for 30:1 T-state PolyhHb batches previously produced in our lab at the bench-top scale. The

TABLE 1 Biophysical properties of PolyhHb

	Pilot T-state PolyhHb ($n = 3$)	Pilot moderate P_{50} PolyhHb ($n = 5$)	Bench-top PolyhHb ($n = 16$) (Cuddington et al., 2021)	Unmodified hHb ($n = 12$) (Cuddington et al., 2021)
Concentration (g/L)	108 ± 5	112 ± 5	107 ± 7	221 ± 12
MetHb level (%)	4.5 ± 1.0 [a]	2.5 ± 0.7[b,c]	5.7 ± 1.7 [a]	2.1 ± 0.7
Yield (%)	34 ± 13	47 ± 5	42 ± 13	N/A
Mass/batch (g)	154 ± 69 [b]	229 ± 23 [b]	12.3 ± 3.8	N/A
D_{eff} (nm)	26.3 ± 5.1[b,c]	30.1 ± 6.0[b,c]	61 ± 15 [a]	5.5 (Xu et al., 1999)
Average MW (kDa)	1010 ± 40[b,c]	1030 ± 30[b,c]	1290 ± 100[a]	64.5 ± 0.1
LMW species (%) (<500 kDa)	3.7 ± 0.7[a]	3.8 ± 0.7[a]	4.6 ± 1.6[a]	100
P_{50} (mm Hg)	32.1 ± 2.0[b,c]	17.3 ± 1.6[a,b,c]	40.8 ± 3.4[a]	13.2 ± 0.6
$k_{o2,off}$ (s^{-1})	32.7 ± 8.6[b]	24.9 ± 4.5[b,c]	46.3 ± 2.0[a]	36.4 ± 1.1
k_{ox} (h^{-1})	0.016 ± 0.006[a]	0.0045 ± 0.0021[a,b,c]	0.020 ± 0.003[a]	0.4321 ± 0.001
k_{Hp-Hb} ($\mu M^{-1}s^{-1}$)	0.012 ± 0.005[a]	0.012 ± 0.006[a]	0.012 ± 0.002[a]	0.34 ± 0.01

Note: Relevant biophysical properties of the eight batches of pilot scale PolyhHb produced in this study as well as the bench-top scale PolyhHb previously produced in our lab (Cuddington et al., 2021).

Abbreviations: LMW, low molecular weight; MW, molecular weight.

[a]Significantly different than unmodified hHb.

[b]Significantly different than bench-top scale T-state PolyhHb.

[c]Significantly different than pilot scale T-state batches.

eight pilot scale batches in this study were further subdivided into three fully T-state batches and five moderate P_{50} batches (where the quaternary state of the Hb in the PolyhHb molecules is between that of T-state and relaxed quaternary state [R-state] Hb).

As mentioned in Section 2, all pilot scale PolyhHb batches produced in this study were concentrated to at least 100 g/L. This is in line with the protocol for PolyhHb production used in our lab for bench-top scale PolyhHb production (Belcher et al., 2020; Cuddington et al., 2020, 2021). Additionally, the average yield for pilot scale PolyhHb batches was 42%, which is identical to the yield of previous bench-top scale 30:1 T-state PolyhHb batches produced in our lab (Cuddington et al., 2021). In summary, the scaled-up PolyhHb production process does not result in a loss in yield compared to the bench-top scale process. On average, the pilot scale process produced 201 g of PolyhHb—16.3× more compared to the benchtop scale—with moderate P_{50} batches producing 18.6× as more compared to the bench-top scale. This exponential increase in PolyhHb production in a single batch helps to both validate the success of the scaled-up process and facilitates the use of the next-generation PolyhHb in future large animal studies.

The most significant difference in protein quantification between pilot scale and bench-top scale PolyhHb process is the percentage of metHb (i.e., metHb level) in the PolyhHb product. The PolyhHb produced in this study consisted of on average 3.2% metHb, which is significantly lower compared to the 30:1 T-state PolyhHb produced previously at the bench-top scale ($p = 0.0014$). Upon analysis of the two pilot scale PolyhHb subgroups, this trend appears to be due to the lower metHb level of the moderate P_{50} pilot scale batches. The

five moderate P_{50} pilot scale batches have a significantly lower metHb level than the three fully T-state batches produced at the pilot scale ($p = 0.015$). This is likely due to two separate factors. First, the pilot-scale PolyhHb synthesis protocol had the purified hHb added directly to the reactor after RBC lysis and filtration through a 500 kDa TFF module. In the bench-top scale synthesis of PolyhHb, the hHb was first filtered through a 500 kDa TFF module and then further concentrated over a 50 kDa TFF module for subsequent storage at −80°C before use. The final concentration step on the 50 kDa TFF module removes excess buffer as well as any proteins <50 kDa, including superoxide dismutase (SOD) which is critical in preventing Hb oxidation. Previous studies have shown that co-polymerizing SOD with PolyhHb can limit the oxidation of PolyhHb, and a similar mechanism is likely at play here to reduce the metHb level of all pilot-scale batches compared to bench-top scale PolyhHb (Bian & Chang, 2015; D'Agnillo & Chang, 1998). Second, previous studies have also shown that the low O_2 affinity (i.e., high P_{50}) of T-state PolyhHb leads to a higher rate of metHb formation compared to species with lower P_{50}s (Belcher et al., 2017, 2018; Gu et al., 2020). This is discussed more in later sections, but for now would help explain the difference in metHb level between moderate P_{50} and fully T-state PolyhHb pilot scale batches.

3.3 | O_2 equilibria

The PolyhHb produced in this study fell into two distinct subgroups: T-state PolyhHb and a moderate O_2 affinity PolyhHb, as shown in
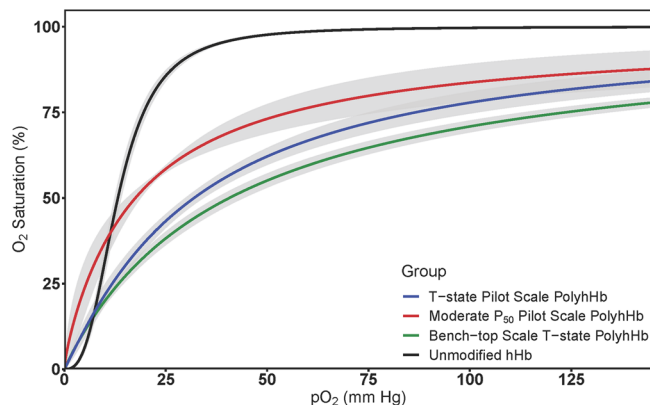
FIGURE 7 Oxygen equilibrium curve (OEC) displaying the O_2 saturation of human hemoglobin (hHb) and polymerized human hemoglobin (PolyhHb) as a function of O_2 tension. The moderate P_{50} pilot scale PolyhHb batches exhibited a significantly higher O_2 affinity compared to fully T-state pilot scale batches and bench-top scale 30:1 T-state PolyhHb batches. The OECs are displayed as averages ± 1 standard deviation shown in gray. All measurements were taken at 37°C and pH 7.4. The number of replicates was listed in Table 1.

FIGURE 8 Molecular weight (MW) distribution of various hemoglobin (Hb)-based O_2 carriers. Bench-top scale polymerized human hemoglobin (PolyhHb) batches exhibited a slight increase in MW compared to the two pilot scale subgroups. All PolyhHbs synthesized in this lab are an order of magnitude larger than previous commercial PolyHbs and 2 orders of magnitude larger than unmodified hHb.

Figure 7. Traditionally, PolyhHb has been synthesized in either a low oxygen affinity T-state (P_{50} > 30 mmHg) or a high oxygen affinity R-state (P_{50} < 2 mmHg). Our lab has shown that moderate P_{50} PolyhHbs (P_{50}: 10–20 mmHg) can be prepared by mixing R-state and T-state fractions together to create a solution with a P_{50} closer to that of unmodified hHb (12.4 mmHg) or RBCs (26 mmHg) (Belcher et al., 2017). In this study, three pilot scale batches were fully deoxygenated before glutaraldehyde addition and throughout the polymerization process resulting in the final PolyhHb product being fully in the T-state. However, five of the batches were not kept under fully anoxic conditions during the polymerization process, with the O_2 tension of the reactor getting as high as 5 mmHg before quenching the polymerization reaction. The marginal amount of O_2 in the system—only about 3% of the O_2 tension of air—alters the quaternary state of the hHb solution to exist in both a partially oxygenated and partially deoxygenated state. This mixture of quaternary states is locked into place during polymerization, creating the moderate P_{50} PolyhHb species observed in this study.

T-state PolyhHb is traditionally used for hemorrhagic shock resuscitation and other therapeutic applications (Cabrales et al., 2009; Muller et al., 2021; Palmer et al., 2011; Yang et al., 2015). The low O_2 affinity of T-state PolyhHb results in the ability of O_2 to be readily offloaded to surrounding tissue to reduce tissue hypoxia (Messmer et al., 2012; Muller et al., 2021). More recent studies have shown that the indiscriminate offloading of O_2 by T-state PolyhHb may not be as beneficial as originally thought (Elmer et al., 2012; Winslow, 2013). For instance, there is an increase in reactive oxygen species (ROS) generation under hyperoxic conditions (Watson et al., 2017). This triggers a cascade of inflammatory response pathways, leading to increased cellular damage (Gozzelino et al., 2010). Additionally, the principle of autoregulation—whereby in the presence of an O_2-rich
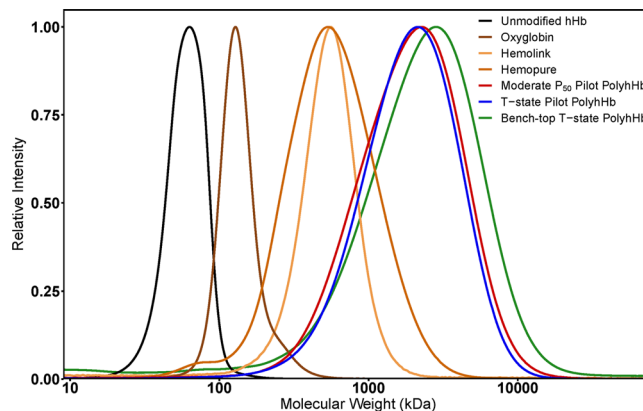
environment, cells will automatically reduce O_2 uptake—has been shown to limit the efficacy of O_2 carriers with P_{50}s significantly higher than RBCs (26 mmHg) (Cabrales et al., 2008). It is for these reasons that moderate P_{50} PolyhHbs show promise as viable RBC substitutes with reduced potential for ROS generation and auto-regulatory response.

3.4 | Size distribution

The size of the PolyhHb synthesized in this study was measured using both DLS and SEC-HPLC and the SEC-HPLC-derived MW results are shown in Figure 8. DLS revealed an average effective diameter (D_{eff}) of 29.6 nm (Figure 9). This is significantly less than PolyhHb of the same crosslink density produced at the bench-top scale (p < 0.001) (Cuddington et al., 2021). Similarly, SEC-HPLC MW analysis revealed that the PolyhHb produced at the pilot-scale is smaller than bench-top scale 30:1 T-state PolyhHb. The pilot scale PolyhHb produced in this study had an average MW of 1020 kDa which is significantly smaller than the 1290 kDa average MW of bench-top scale PolyhHb (p < 0.001). The PolyhHb synthesized in this study is still classified as an ultrahigh MW (MW ≥ 1000 kDa), high-purity PolyhHb so the size disparity is not of concern.

The size difference between pilot scale and bench-top scale batches is likely due to mixing differences between the pilot-scale reactor system compared to the bench-top scale reactor system. Bench-top PolyhHb syntheses used a stir bar as the agitator for mixing and the reactor has no baffles, while the pilot-scale reactor is a baffled CSTR with an impeller, so it inherently generates more uniform mixing. Ostwald ripening is a well-described process whereby particles in solution are more likely to interact with larger particles over smaller ones. In a reactor set-up where mixing is not as uniform
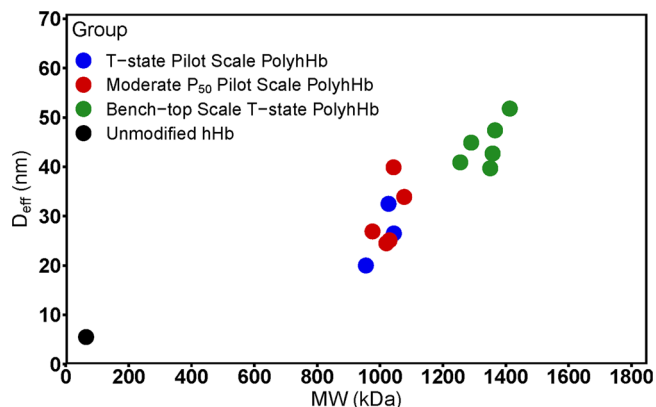
FIGURE 9 Effective diameter versus average molecular weight (MW). Bench-top scale polymerized human hemoglobin (PolyhHb) batches exhibited a higher average MW and D_{eff}. Pilot scale PolyhHb does not exhibit a difference in between subgroups.

FIGURE 10 Auto-oxidation kinetics of human hemoglobin (hHb) and polymerized human hemoglobin (PolyhHb). The decrease in [Fe^{2+}] was linearized according to first-order rate kinetics. T-state PolyhHb—regardless of scale—exhibited a k_{ox} ~4× higher than that of the moderate P_{50} pilot scale PolyhHb. There was no significant difference in k_{ox} between pilot and bench-top scale T-state PolyhHb. The number of replicates was listed in Table 1.

as in a CSTR, it is to be expected that Ostwald ripening will occur more frequently, resulting in a more bimodal distribution of Hb polymers. This is opposed to a perfectly mixed system, where there should be a more even distribution of polymer sizes, which would explain the smaller MW of the PolyhHb produced at the pilot-scale compared to bench-top scale. The optimal mixing of the pilot scale reactor is confirmed in the computational fluid modeling described in a later section.

3.5 | Auto-oxidation

Similar to the discussion regarding PolyhHb oxygen affinity, the auto-oxidation rate constant of pilot scale PolyhHbs produced in this study fell into two distinct subgroups. The auto-oxidation rate constant and oxygen affinity appear to be mildly correlated in Figure 10. Every pilot scale batch with a moderate P_{50} resulted in a lower auto-oxidation rate constant, and most of the T-state PolyhHb batches fell into the higher auto-oxidation rate constant group. Examining the subgroups as a whole, the moderate P_{50} pilot scale PolyhHbs exhibited statistically significantly lower auto-oxidation rate constants than fully T-state pilot scale PolyhHbs ($p = 0.0065$). This phenomenon was observed previously, with R-state PolyhHb exhibiting a lower auto-oxidation rate constant compared to T-state PolyhHb (Belcher et al., 2018).

The k_{ox} for both pilot scale groups in this study was lower compared to other HBOCs in the literature. Unmodified hHb has been shown to have a k_{ox} of 0.043 h^{-1}, which is 2× higher than the pilot scale T-state PolyhHb group and ~9× higher than the moderate P_{50} pilot scale PolyhHb group. Furthermore, the commercial PolyhHb PolyHeme® (Northfield Labs) was shown to have a k_{ox} of 0.26 h^{-1}, which is 10-fold and 45-fold higher than the pilot scale PolyhHbs synthesized in this study (Meng et al., 2018). The low concentration of LMW Hb polymers (<500 kDa) present in the pilot scale materials is thought to be the source of the lower auto-oxidation rate constant
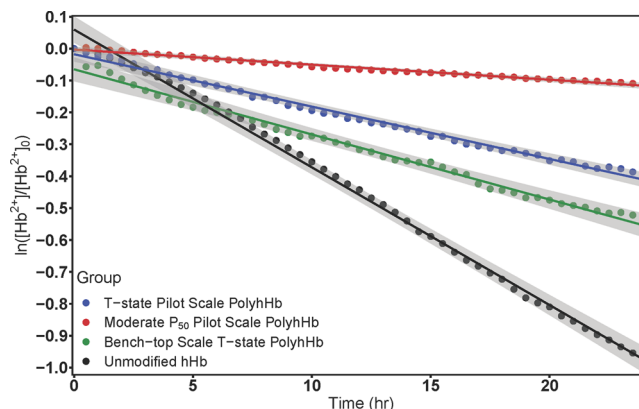
compared to prior generations of HBOCs. Previous studies from our lab have shown a positive correlation between the concentration of low MW species in the PolyhHb solution and the auto-oxidation rate constant (Belcher et al., 2020). All PolyhHbs synthesized in this study had less than 1/10 of the LMW species (<500 kDa) that were present in previous commercial HBOCs, so it makes sense for the auto-oxidation rate constant to also be an order of magnitude lower as well.

The lower auto-oxidation rate constant is important for two major reasons. The first is that a lower rate of auto-oxidation will correspond to a greater amount of ferrous PolyhHb being capable of carrying and offloading O_2 while in circulation. When ferrous PolyhHb oxidizes, it converts into the ferric state (i.e., metHb), and is no longer able to bind and release O_2. For HBOCs with high k_{ox} values, the O_2-carrying capacity of the solution drops off rapidly as the ferrous HBOC converts to metHb and therefore loses functionality over a very short time period. In contrast, low k_{ox} HBOCs, such as the pilot-scale PolyhHb produced in this study, do not have this problem and remain functional for a much longer period of time, making them significantly more viable as an O_2 therapeutic. Additionally, the Fe^{3+} in metHb is a strong oxidizer, which gives it the ability to produce ROS that is cytotoxic (Smith & McCulloh, 2015). This further supports the advantages of the low k_{ox} HBOCs produced in this study as these molecules will be less likely to catalyze ROS production and elicit cellular toxicity.

3.6 | Deoxygenation kinetics

Figure 11 shows the kinetics of O_2 offloading by PolyhHb produced at the pilot-scale was slower than T-state PolyhHb produced at the bench-top scale ($p < 0.001$) (Cuddington et al., 2021). Initially, this

was assumed to be related to the lower average P_{50} of pilot scale PolyhHb compared to bench-top scale PolyhHb. Previous studies have shown that $k_{o2,off}$ decreases with a decrease in P_{50} with T-state PolyhHb having a $k_{o2,off} > 41\,s^{-1}$ and R-state PolyhHb having a $k_{o2,off} < 30\,s^{-1}$. This was not the case in this study though with two of the three batches of T-state PolyhHb having a $k_{o2,off}$ less than that of hHb ($41\,s^{-1}$) (Belcher et al., 2020; Cuddington et al., 2021). The initial hypothesis of O_2 affinity and O_2 offloading rate constant being related falls apart even further when considering the moderate P_{50} pilot scale batches of PolyhHb. Despite all five moderate P_{50} PolyhHb pilot scale batches being closer in O_2 affinity to hHb than R-state

FIGURE 11 Oxygen (O_2) offloading kinetics of human hemoglobin (hHb) and polymerized human hemoglobin (PolyhHb). Normalized O_2 offloading kinetics. While T-state PolyhHb trended towards a higher $k_{o2,off}$, and moderate P_{50} PolyhHb trended towards a lower $k_{o2,off}$, there was no correlation found in this study. Bench-top scale T-state PolyhHb had a significantly higher $k_{o2,off}$ than both pilot scale groups. The number of replicates was listed in Table 1.

PolyhHb, they all have a $k_{o2,off}$ resembling that of R-state PolyhHb (~23 s^{-1}), not hHb (Belcher et al., 2017, 2020). These results speak well to the potential ability of pilot-scale PolyhHb to carry and offload O_2 while preventing autoregulation; however, the cause for the decoupling of O_2 affinity and O_2 offloading rate constant is still yet to be determined.

3.7 | Hp binding kinetics

The plot of the pseudo-first-order rate constant as a function of Hb concentration for Hp binding ($k_{Hp\text{-}Hb}$) to the PolyhHbs produced in this study is shown in Figure 12b and was identical to bench-top scale PolyhHb (Cuddington et al., 2021). A representative kinetic time course for PolyhHb binding to Hp shows the overlap between PolyhHb groups in Figure 12a. The reason for the difference in Hp binding rates between hHb and all PolyhHb groups is likely due to the increased measures taken to remove LMW Hb species (<500 kDa) from the final PolyhHb product. Both the pilot-scale PolyhHb produced in this study, and the bench-top-scale PolyhHb produced previously were subject to diafiltration over a 500 kDa membrane. Hp can only bind to cell-free Hb and LMW Hb species (Schaer et al., 2016; Silverman & Weiskopf, 2009). Therefore, it is logical that thorough removal of such species through a 500 kDa TFF membrane should drastically reduce the Hp binding rate to PolyhHb. This is supported by the fact that both pilot-scale and bench-top scale PolyhHb have less than 5% LMW species in solution, so they should both have similar, trivially small $k_{Hp\text{-}Hb}$ values compared to hHb.

Because Hp is the native hHb clearance protein, a high level of Hp-binding would imply the presence of large quantities of cytotoxic Hb species. The elimination of such species would therefore lead to a
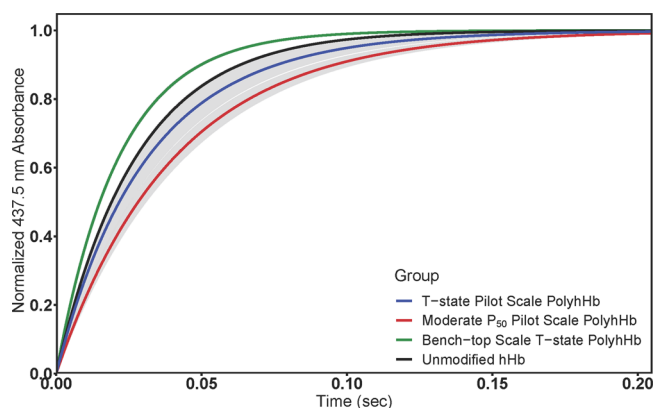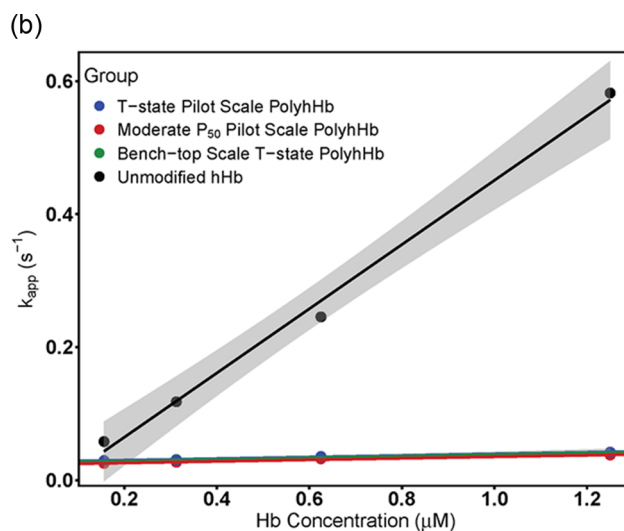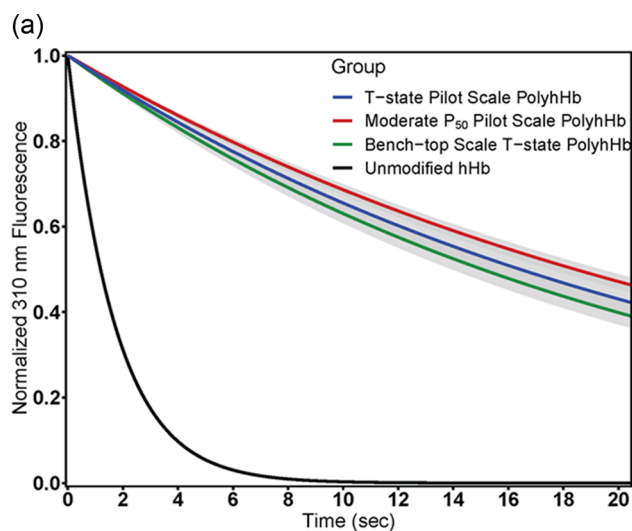

FIGURE 12 Hp binding kinetics to human hemoglobin (hHb) and polymerized human hemoglobin (PolyhHb). Representative first-order kinetics for the reaction of 0.25 μM Hp with 1.25 μM PolyhHb (a) and linearization of the apparent first-order rate constant as a function of [Hb] (b). There was no significant difference between any groups or batches of PolyhHb in either the first or second-order rate kinetics. All measurements were taken using a 285 nm excitation wavelength and a 310 nm emission wavelength. The number of replicates was listed in Table 1.
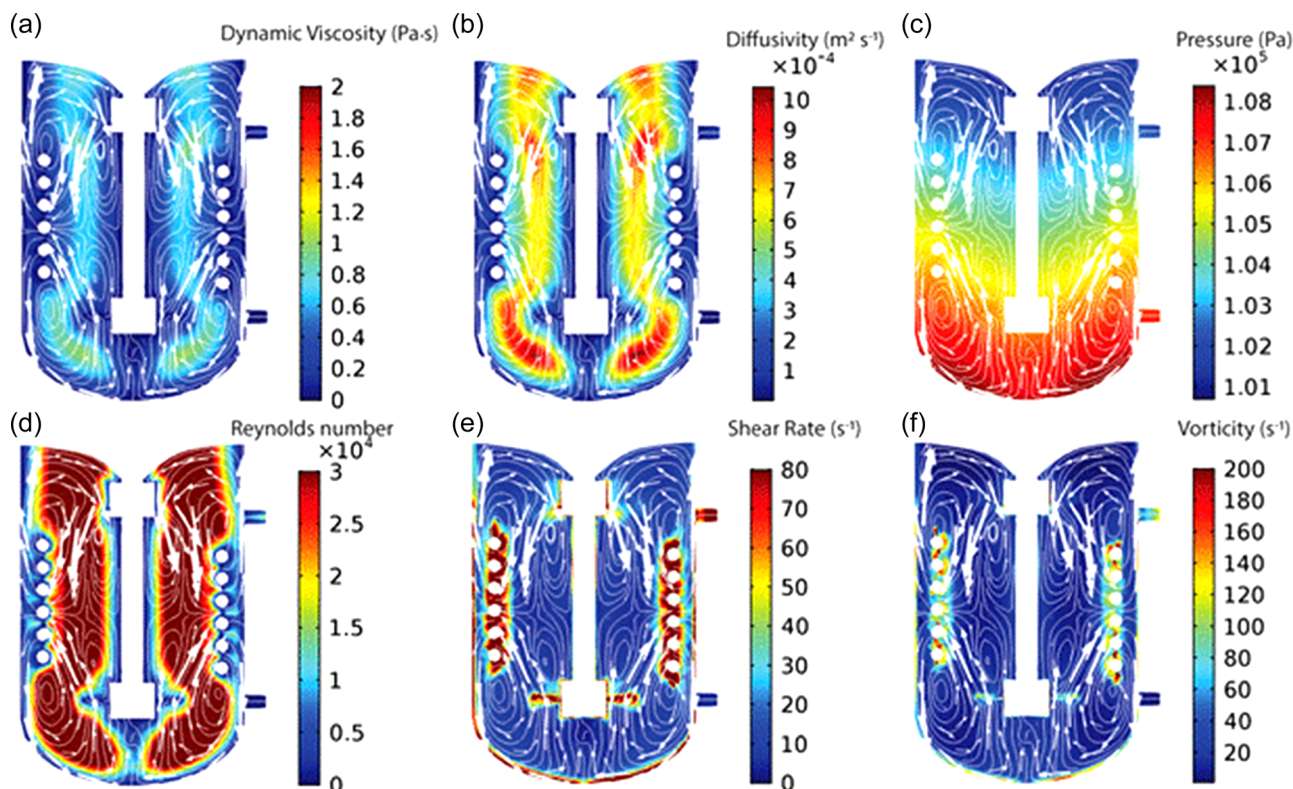
FIGURE 13 Various turbulence parameters with streamlines in the continuous stirred tank reactor vessel. Dynamic viscosity (a), eddy diffusivity (b), pressure (c), Reynolds number (d), shear rate (e), and vorticity (f) in the reactor vessel were all modeled using computational fluid dynamics.

decrease in k_{Hp-Hb}. This can be taken to mean that k_{Hp-Hb} is inversely proportional to the safety of the PolyhHb if it were to be transfused since a low Hp binding constant would imply less cytotoxic potential. The k_{Hp-Hb} of the PolyhHb produced in this study is trivial and 100-fold less than that of unmodified hHb, alluding to its safety as a potential RBC substitute.

3.8 | Mixing modeling

Figure 13a shows the dynamic viscosity distribution in the pilot scale reactor in the case of four-bladed pitched impeller at a revolution speed of 130 rpm. The dynamic viscosity in bulk solution (0.6–1.1 Pa s) was slightly higher than that in the regions proximate to the interior wall, coil, and impellers (0 < 0.6 Pa s) of the reactor. Figure 13b shows the eddy diffusivity profile in the reactor during the polymerization process. The diffusivity was observed to be maximum (0.001 m^2 s^{-1}) at the surface of the impeller, which decreased radially towards the vessel wall. It is obvious that there was sufficient vertical and horizontal diffusion in the bulk solution (0.0005–0.001 m^2 s^{-1}). The pressure distribution was shown in Figure 13c and ranged from 101 to 108 kPa. Figure 13d shows the Reynolds number (Re) distribution in the stirred tank reactor. It was observed that turbulent flow was fully developed in the bulk solution (Re > 4000). The solution proximate to the cooling coil and wall exhibited transient

flow behavior given that the Re ranged from 2000 to 4000. As expected, the region near the cooling coil and interior wall was not well mixed compared to the bulk of the reactor.

Figure 13e,f shows that the shear rate and vorticity at a rotational speed of 130 rpm were higher near the impeller than in the bulk solution. It was found that the pitched turbine impeller can be used to achieve adequate mixing in the stirred vessel since negligible vorticity was generated. Vigorous mixing with turbulent flow assisted in preventing vortex formation. Overall, we demonstrate the usefulness of CFD modeling for evaluating the mixing performance in the reactor. Future work should model heat transfer to calculate the temperature profile in the reactor during the polymerization process.

4 | CONCLUSIONS

This study serves as a proof of concept that a high MW next-generation PolyhHb with limited LMW Hb species can be produced at the pilot scale (200–300 g of PolyhHb product). Bench-top and pilot-scale PolyhHb processes exhibited nearly identical protein yields. Additionally, pilot-scale PolyhHb produced in this study was shown to have a lower metHb level and auto-oxidation rate constant compared to bench-top scale PolyhHb. We also demonstrated that PolyhHb could be produced in either the low O$_2$ affinity T-state or at

a moderate P_{50} making it possible to produce an HBOC that can readily offload O_2 without possible concerns over autoregulation. Optimized mixing parameters most likely lead to the pilot-scale PolyhHb being smaller compared to previous bench-top scale PolyhHbs. Furthermore, the pilot scale PolyhHbs produced in this exhibited a low Hp binding rate constant, further indicating the potential safety of the material.

AUTHOR CONTRIBUTIONS

ACKNOWLEDGMENTS

DATA AVAILABILITY STATEMENT

The data that support the findings of this study are available from the corresponding author upon reasonable request.

ORCID

Clayton T. Cuddington http://orcid.org/0000-0001-8739-2155
Donald A. Belcher http://orcid.org/0000-0002-7633-6219
Xiangming Gu http://orcid.org/0000-0001-9096-5911

REFERENCES

Alayash, A. I. (2000). Hemoglobin-based blood substitutes and the hazards of blood radicals. *Free Radical Research*, *33*(4), 341–348. https://doi.org/10.1080/10715760000300881

Alayash, A. I., Summers, A. G., Wood, F., & Jia, Y. (2001). Effects of glutaraldehyde polymerization on oxygen transport and redox properties of bovine hemoglobin. *Archives of Biochemistry and Biophysics*, *391*(2), 225–234. https://doi.org/10.1006/abbi.2001.2426

American Red Cross. (2022a). *Red cross declares first-ever blood crisis amid omicron surge*. https://www.redcross.org/about-us/news-and-events/press-release/2022/blood-donors-needed-now-as-omicron-intensifies.html

American Red Cross. (2022b). *What to know about the coronavirus and blood donation*. https://www.redcrossblood.org/donate-blood/dlp/coronavirus–covid-19–and-blood-donation.html

Arifin, D. R., & Palmer, A. F. (2003). Determination of size distribution and encapsulation efficiency of liposome-encapsulated hemoglobin blood substitutes using asymmetric flow field-flow fractionation coupled with multi-angle static light scattering. *Biotechnology Progress*, *19*(6), 1798–1811. https://doi.org/10.1021/bp034120x

Belcher, D. A., Banerjee, U., Baehr, C. M., Richardson, K. E., Cabrales, P., Berthiaume, F., & Palmer, A. F. (2017). Mixtures of tense and relaxed state polymerized human hemoglobin regulate oxygen affinity and tissue construct oxygenation. *PLoS One*, *12*(10), 1–22. https://doi.org/10.1371/journal.pone.0185988

Belcher, D. A., Cuddington, C. T., Martindale, E. L., Pires, I. S., & Palmer, A. F. (2020). Controlled polymerization and ultrafiltration increase the consistency of polymerized hemoglobin for use as an oxygen carrier. *Bioconjugate Chemistry*, *31*(3), 605–621. https://doi.org/10.1021/acs.bioconjchem.9b00766

Belcher, D. A., Ju, J. A., Baek, J. H., Yalamanoglu, A., Buehler, P. W., Gilkes, D. M., & Palmer, A. F. (2018). The quaternary state of polymerized human hemoglobin regulates oxygenation of breast cancer solid tumors: A theoretical and experimental study. *PLoS One*, *13*(2):e0191275. https://doi.org/10.1371/journal.pone.0191275

Bian, Y., & Chang, T. M. S. (2015). A novel nanobiotherapeutic poly-[hemoglobin-superoxide dismutase-catalase-carbonic anhydrase] with no cardiac toxicity for the resuscitation of a rat model with 90 minutes of sustained severe hemorrhagic shock with loss of 2/3 blood volume. *Artificial Cells Blood Substitutes and Biotechnology*, *43*(1), 1–9. https://doi.org/10.3109/21691401.2014.964554

Bucci, E., Kwansa, H., Koehler, R. C., & Matheson, B. (2008). Development of zero-link polymers of hemoglobin, which do not extravasate and do not induce pressure increases upon infusion. *Artificial Cells Blood Substitutes and Biotechnology*, *35*(1), 11–18.

Buehler, P. W., Zhou, Y., Cabrales, P., Jia, Y., Sun, D., Harris, D., Tsai, A., Intaglietta, M., & Palmer, A. (2010). Synthesis, biophysical properties and pharmacokinetics of ultrahigh molecular weight tense and relaxed state polymerized bovine hemoglobins. *Biomaterials*, *31*(13), 3723–3735. https://doi.org/10.1016/j.biomaterials.2010.01.072

Butt, O. I., Buehler, P. W., & D'Agnillo, F. (2011). Blood-brain barrier disruption and oxidative stress in guinea pig after systemic exposure to modified cell-free hemoglobin. *American Journal of Pathology*, *178*(3), 1316–1328. https://doi.org/10.1016/j.ajpath.2010.12.006

Cabrales, P., Tsai, A. G., & Intaglietta, M. (2007). Is resuscitation from hemorrhagic shock limited by blood oxygen-carrying capacity or blood viscosity? *Shock*, *27*(4), 380–389. https://doi.org/10.1097/01.shk.0000239782.71516.ba

Cabrales, P., Tsai, A. G., & Intaglietta, M. (2008). Modulation of perfusion and oxygenation by red blood cell oxygen affinity during acute anemia. *American Journal of Respiratory Cell and Molecular Biology*, *38*(3), 354–361. https://doi.org/10.1165/rcmb.2007-0292OC

Cabrales, P., Tsai, A. G., & Intaglietta, M. (2009). Polymerized bovine hemoglobin can improve small-volume resuscitation from hemorrhagic shock in hamsters. *Shock*, *31*(3), 300–307. https://doi.org/10.1097/SHK.0b013e318180ff63

Chang, T. M. S. (1971). Stablisation of enzymes by microencapsulation with a concentrated protein solution or by microencapsulation followed by cross-linking with glutaraldehyde. *Biochemical and Biophysical Research Communications*, *44*(6), 1531–1536. https://doi.org/10.1016/S0006-291X(71)80260-7

Chang, T. M. S., Bülow, L., Jahr, J., Sakai, H., & Yang, C. (2021). *Nanobiotherapeutic based blood substitutes*. World Scientific. https://doi.org/10.1142/12054

Chen, G., & Palmer, A. F. (2009). Hemoglobin-based oxygen carrier and convection enhanced oxygen transport in a hollow fiber bioreactor. *Biotechnology and Bioengineering*, *102*(6), 1603–1612. https://doi.org/10.1002/bit.22200

Chen, J. Y., Scerbo, M., & Kramer, G. C. (2009). A review of blood substitutes: Examining the history, clinical trial results, and ethics of hemoglobin-based oxygen carriers. *Clinics*, *64*(8), 803–813. https://doi.org/10.1590/S1807-59322009000800016

Cuddington, C.T., Moses, S., Belcher, D. A., Ramesh, N., & Palmer, A. F. (2020). Next-generation polymerized human hemoglobins in hepatic bioreactor simulations. *Biotechnology Progress*, *36*(3):e2958. https://doi.org/10.1002/btpr.2958

Cuddington, C. T., Wolfe, S. R., & Palmer, A. F. (2021). Biophysical properties of tense quaternary state polymerized human

hemoglobins bracketed between 500 kDa and 0.2 μm in size. *Biotechnology Progress*, 38(1), 1–8. https://doi.org/10.1002/btpr.3219

Cullison, M., Mahon, R., McGwin, G., McCarron, R., Browning, R., & Auker, C. (2019). Blood transfusions, blood storage, and correlation with elevated pulmonary arterial pressures. *Transfusion*, 59(4), 1259–1266. https://doi.org/10.1111/TRF.15122

D'Agnillo, F., & Chang, T. M. S. (1998). Polyhemoglobin-superoxide dismutase catalase as a blood substitute with antioxidant properties. *Nature Biotechnology*, 16(7), 667–671. https://doi.org/10.1038/nbt0798-667

Elmer, J., Alam, H. B., & Wilcox, S. R. (2012). Hemoglobin-based oxygen carriers for hemorrhagic shock. *Resuscitation*, 83(3), 285–292. https://doi.org/10.1016/j.resuscitation.2011.09.020

Faghih, M.M., & Sharp, M. K. (2019). Modeling and prediction of flow-induced hemolysis: A review. *Biomechanics and Modeling in Mechanobiology*, 18(4), 845–881. https://doi.org/10.1007/s10237-019-01137-1

Gaur, U., Sahoo, S. K., De, T. K., Ghosh, P. C., Maitra, A., & Ghosh, P. K. (2000). Biodistribution of fluoresceinated dextran using novel nanoparticles evading reticuloendothelial system. *International Journal of Phamaceutics*, 202(1–2), 1–10. https://doi.org/10.1016/S0378-5173(99)00447-0

Gibson, B. Q. H., & Roughton, F. J. W. (1956). The kinetics and equilibria of the reactions of nitric oxide with sheep haemoglobin. *Journal of Physiology*, 136(3), 507–526.

Glynn, S. A., Busch, M. P., Schreiber, G. B., Murphy, E. L., Wright, D. J., Tu, Y., & Kleinman, S. H. (2003). Effect of a national disaster on blood supply and safety: The September 11 experience. *JAMA*, 289(17), 2246–2253.

Gozzelino, R., Jeney, V., & Soares, M. P. (2010). Mechanisms of cell protection by heme oxygenase-1. *Annual Review of Pharmacology and Toxicology*, 50(1), 323–354. https://doi.org/10.1146/annurev.pharmtox.010909.105600

Greenburg, A. G. (1996). Benefits and risks of blood transfusion in surgical patients. *World Journal of Surgery*, 20, 1189–1193.

Gu, X., Bolden-Rush, C., Cuddington, C. T., Belche, D. A., Savla, C., Pires, I. S., & Palmer, A. F. (2020). Comprehensive characterization of tense and relaxed quaternary state glutaraldehyde polymerized bovine hemoglobin as a function of cross-link density. *Biotechnology and Bioengineering*, 117(8), 2362–2376. https://doi.org/10.1002/bit.27382

Guillochon, D., Esclade, L., Remy, M. H., & Thomas, D. (1981). Studies on haemoglobin immobilized by cross-linking with glutaraldehyde cross-linked soluble polymers and artificial membranes. *Biochimica et Biophysica Acta*, 670(3), 332–340. https://doi.org/10.1016/0005-2795(81)90105-7

Guillochon, D., Vijayalakshmi, M. W., Thiam-Sow, A., & Thomas, D. (1986). Effect of glutaraldehyde on hemoglobin: Functional aspects and Mossbauer parameters. *Biochemistry and Cell Biology*, 64(1), 29–37. https://doi.org/10.1139/o86-005

Gustafson, H. H., Holt-Casper, D., Grainger, D. W., & Ghandehari, H. (2015). Nanoparticle uptake: The phagocyte problem. *Nano Today*, 10(4), 487–510. https://doi.org/10.1016/j.nantod.2015.06.006

Harris, D. R., & Palmer, A. F. (2008). Modern cross-linking strategies for synthesizing acellular hemoglobin-based oxygen carriers. *Biotechnology Progress*, 24(6), 1215–1225. https://doi.org/10.1002/btpr.85.Modern

Holcomb, J. B., Tilley, B. C., Baraniuk, S., Fox, E. E., Wade, C. E., Podbielski, J. M., del Junco, D. J., Brasel, K. J., Bulger, E. M., Callcut, R. A., Cohen, M. J., Cotton, B. A., Fabian, T. C., Inaba, K., Kerby, J. D., Muskat, P., O'Keeffe, T., Rizoli, S., Robinson, B. R. H, ... PROPPR Study Group. (2015). Transfusion of plasma, platelets, and red blood cells in a 1:1:1 vs a 1:1:2 ratio and mortality in patients with severe trauma. *Journal of the American Medical Association*, 313(5), 471–482. https://doi.org/10.1001/jama.2015.12

Jahr, J. S., MacKenzie, C., Pearce, L. B., Pitman, A., & Greenburg, A. G. (2008). HBOC-201 as an alternative to blood transfusion: Efficacy and safety evaluation in a multicenter phase III trial in elective orthopedic surgery. *The Journal of Trauma*, 64(6), 1484–1497. https://doi.org/10.1097/TA.0b013e318173a93f

Kavdia, M., Tsoukias, N. M., & Popel, A. S. (2002). Model of nitric oxide diffusion in an arteriole: Impact of hemoglobin-based blood substitutes. *American Journal of Physiology—Heart and Circulatory Physiology*, 282(6), H2245–H2253.

Kim, H. W., & Greenburg, A. G. (2004). Artificial oxygen carriers as red blood cell substitutes: A selected review and current status. *Artificial Organs*, 28(9), 813-828. https://doi.org/10.1111/j.1525-1594.2004.07345.x

McCarthy, M. R., Vandegriff, K. D., & Winslow, R. M. (2001). The role of facilitated diffusion in oxygen transport by cell-free hemoglobins: Implications for the design of hemoglobin-based oxygen carriers. *Biophysical Chemistry*, 92(1–2), 103–117. https://doi.org/10.1016/S0301-4622(01)00194-6

Meng, F., Kassa, T., Jana, S., Wood, F., Zhang, X., Jia, Y., D'Agnillo, F., & Alayash, A. I. (2018). Comprehensive biochemical and biophysical characterization of hemoglobin-based oxygen carrier therapeutics: All HBOCs are not created equally. *Bioconjugate Chemistry*, 29(5), 1560–1575. https://doi.org/10.1021/acs.bioconjchem.8b00093

Messmer, C., Yalcin, O., Palmer, A. F., & Cabrales, P. (2012). Small-volume resuscitation from hemorrhagic shock with polymerized human serum albumin. *American Journal of Emergency Medicine*, 30(8), 1336–1346. https://doi.org/10.1016/J.AJEM.2011.09.018

Moore, E. E., Moore, F. A., Fabian, T. C., Bernard, A. C., Fulda, G. J., Hoyt, D. B., Duane, T. M., Weireter, L. J., Jr, Gomez, G. A., Cipolle, M. D., Rodman, G. H., Jr, Malangoni, M. A., Hides, G. A., Omert, L. A., & Gould, S. A. (2009). Human polymerized hemoglobin for the treatment of hemorrhagic shock when blood is unavailable: The USA multicenter trial. *Journal of the American College of Surgeons*, 208(1), 1–13.

Muller, C. R., Courelli, V., Lucas, A., Williams, A. T., Li, J. B., Dos Santos, F., Cuddington, C. T., Moses, S. R., Palmer, A. F., Kistler, E. B., & Cabrales, P. (2021). Resuscitation from hemorrhagic shock after traumatic brain injury with polymerized hemoglobin. *Scientific Reports*, 11(1), 2509.

Myburgh, J. A., Finfer, S., Bellomo, R., Billot, L., Cass, A., Gattas, D., Glass, P., Lipman, J., Liu, B., McArthur, C., McGuinness, S., Rajbhandari, D., Taylor, C. B., Webb, S. A. R., CHEST Investigators, & Australian and New Zealand Intensive Care Society Clinical Trials Group. (2012). Hydroxyethyl starch or saline for fluid resuscitation in intensive care. *New England Journal of Medicine*, 367(20), 1901–1911. https://doi.org/10.1056/nejmoa1209759

Palmer, A. F., Sun, G., & Harris, D. R. (2009). Tangential flow filtration of hemoglobin. *Biotechnology Progress*, 25(1), 189–199. https://doi.org/10.1002/btpr.119

Palmer, A. F., Zhang, N., Zhou, Y., Harris, D. R., & Cabrales, P. (2011). Small-volume resuscitation from hemorrhagic shock using high-molecular-weight tense-state polymerized hemoglobins. *The Journal of Trauma*, 71(4), 798–807. https://doi.org/10.1097/TA.0b013e3182028ab0

Pires, I. S., & Palmer, A. F. (2021). Selective protein purification via tangential flow filtration—Exploiting protein-protein complexes to enable size-based separations. *Journal of Membrane Science*, 618, 118712. https://doi.org/10.1016/j.memsci.2020.118712

Schaer, C. A., Deuel, J. W., Schildknecht, D., Mahmoudi, L., Garcia-Rubio, I., Owczarek, C., Schauer, S., Kissner, R., Banerjee, U., Palmer, A. F., Spahn, D. R., Irwin, D. C., Vallelian, F., Buehler, P. W., & Schaer, D. J. (2016). Haptoglobin preserves vascular nitric oxide signaling during hemolysis. *American Journal of Respiratory and Critical Care Medicine*,

193(10), 1111–1122. https://doi.org/10.1164/rccm.201510-2058OC

Silverman, T.A., & Weiskopf, R. B. (2009). Hemoglobin-based oxygen carriers: Current status and future directions. Transfusion, 49(11), 2495–2515. https://doi.org/10.1111/j.1537-2995.2009.02356.x

Smith, A., & McCulloh, R. J. (2015). Hemopexin and haptoglobin: Allies against heme toxicity from hemoglobin not contenders. Frontiers in Physiology, 6, 187. https://doi.org/10.3389/fphys.2015.00187

Stowell, C. P., Levin, J., Spiess, B. D., & Winslow, R. M. (2001). Progress in the Development of RBC substitutes. Transfusion, 41(2), 287–299.

Watson, C. J. E., Kosmoliaptsis, V., Randle, L. V., Gimson, A. E., Brais, R., Klinck, J. R., Hamed, M., Tsyben, A., & Butler, A. J. (2017). Normothermic perfusion in the assessment and preservation of declined livers before transplantation: Hyperoxia and vasoplegia-important lessons from the first 12 cases. Transplantation, 101(5), 1084–1098.

Winslow, R. M. (2007). Red cell substitutes. Seminars in Hematology, 44(1), 51–59. https://doi.org/10.1053/J.SEMINHEMATOL.2006.09.013

Winslow, R. M. (2013). Oxygen: The poison is in the dose. Transfusion, 53(2), 424–437. https://doi.org/10.1111/J.1537-2995.2012.03774.X

Xu, H., Bjerneld, E. J., Käll, M., & Börjesson, L. (1999). Spectroscopy of single hemoglobin molecules by surface enhanced Raman scattering. Physics Review Letter, 83(21), 4357–4360. https://doi.org/10.1103/PhysRevLett.83.4357

Yang, G., Sau, C., Lai, W., Cichon, J., & Li, W. (2015). Cardiac function during resuscitation from hemorrhagic shock with polymerized bovine hemoglobin-based oxygen therapeutic. Artificial Cells Blood Substitutes and Biotechnology, 344(6188), 1173–1178. https://doi.org/10.1126/science.1249098.Sleep

Zhang, N., Jia, Y., Chen, G., Cabrales, P., & Palmer, A. F. (2011). Biophysical properties and oxygenation potential of high-molecular-weight glutaraldehyde-polymerized human hemoglobins maintained in the tense and relaxed quaternary states. Tissue Engineering. Part A, 17(7–8), 927–940. https://doi.org/10.1089/ten.tea.2010.0353

SUPPORTING INFORMATION

Additional supporting information can be found online in the Supporting Information section at the end of this article.